



In Vitro, *In Silico*, and *In Vivo* Analyses of Novel Aromatic Amidines against *Trypanosoma cruzi*

Camila C. Santos,^a Jéssica R. Lionel,^a Raiza B. Peres,^a Marcos M. Batista,^a Patrícia B. da Silva,^a Gabriel M. de Oliveira,^a Cristiane F. da Silva,^a Denise G. J. Batista,^a Sandra Maria O. Souza,^b Carolina H. Andrade,^c Bruno J. Neves,^c Rodolpho C. Braga,^c Donald A. Patrick,^d Svetlana M. Bakunova,^d Richard R. Tidwell,^d Maria de Nazaré C. Soeiro^a

^aLaboratory of Cellular Biology (LBC), Oswaldo Cruz Institute (Fiocruz), Rio de Janeiro, RJ, Brazil

^bLaboratory of Structural Biology (LBE), Oswaldo Cruz Institute (Fiocruz), Rio de Janeiro, RJ, Brazil

^cLaboratory for Molecular Modeling and Drug Design (LabMol), Faculdade de Farmácia, Universidade Federal de Goiás, Goiânia, Brazil

^dDepartment of Pathology and Laboratory Medicine, University of North Carolina School of Medicine, Chapel Hill, North Carolina, USA

ABSTRACT Five bis-arylimidamides were assayed as anti-*Trypanosoma cruzi* agents by *in vitro*, *in silico*, and *in vivo* approaches. None were considered to be pan-assay interference compounds. They had a favorable pharmacokinetic landscape and were active against trypomastigotes and intracellular forms, and in combination with benznidazole, they gave no interaction. The most selective agent (28SMB032) tested *in vivo* led to a 40% reduction in parasitemia (0.1 mg/kg of body weight/5 days intraperitoneally) but without mortality protection. *In silico* target fishing suggested DNA as the main target, but ultrastructural data did not match.

KEYWORDS Chagas disease, arylimidamides, experimental chemotherapy, *in vivo*

According to the World Health Organization (1), more than 6 million people worldwide are infected with *Trypanosoma cruzi*, the etiological agent of Chagas disease (CD), and less than 1% are treated with the current available drugs, nifurtimox and benznidazole (Bz), which exhibit several limitations, including low efficacy at the later disease stage and toxic events (2, 3). There is an urgent need to develop alternatives for the treatment of this silent and progressive neglected agent of disease. Aromatic diamidines have antitumor and broad-spectrum antimicrobial activities, and some of their analogues, such as arylimidamides (AIAs), have greater potency and selectivity against intracellular parasites (4). Thus, our aim was to evaluate the biological effects of five novel bis-AIAs (Table 1) against *T. cruzi* by integrating *in vitro*, *in silico*, and *in vivo* tools. 2EVK008, 36DAP015, 27SMB078, 28SMB032, and 31DAP069 were synthesized (see Fig. S1 in the supplemental material) as reported previously (5–8), and experimental details are provided in the supplemental material.

The first evaluation of bloodstream trypomastigotes (BTs) from the Y strain (discrete typing unit II [DTU II]) showed that 4 out of 5 compounds are more active than Bz after 24 h of incubation. 2EVK008, 31DAP069, and 36DAP015 also are “fast killers” (with a 50% effective concentration [EC₅₀] of <10 μM after 2 h of incubation), displaying high potency (Table 1). The activity against intracellular forms (e.g., the Tulahuen strain [DTU VI], which expresses the *Escherichia coli* β-galactosidase [β-Gal] gene) demonstrated that 2EVK008, 28SMB032, 36DAP015, and 31DAP069 have EC₅₀s lower than that of Bz (Table 1). 31DAP069 and 36DAP015 exhibit considerable mammalian host cell toxicity (with a 50% lethal concentration [LC₅₀] ranging between 9 and 12 μM against mouse L929 fibroblasts), while 28SMB032 is less toxic according to alamarBlue assays (9) and exhibits high selectivity indexes (SIs) of >54 and 285 for BT and intracellular forms, respectively. The trypanocidal effect of 28SMB032 was confirmed toward different

Received 26 October 2017 Accepted 20 November 2017

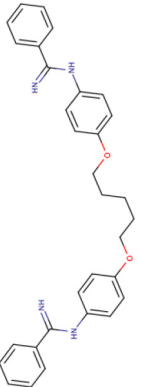
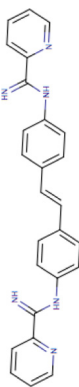
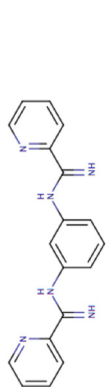
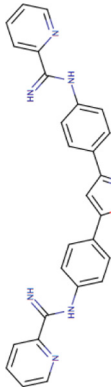
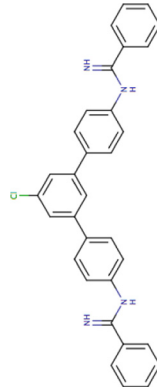
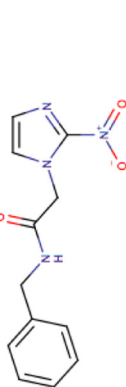
Accepted manuscript posted online 4 December 2017

Citation Santos CC, Lionel JR, Peres RB, Batista MM, da Silva PB, de Oliveira GM, da Silva CF, Batista DGJ, Souza SMO, Andrade CH, Neves BJ, Braga RC, Patrick DA, Bakunova SM, Tidwell RR, Soeiro MDNC. 2018. *In vitro*, *in silico*, and *in vivo* analyses of novel aromatic amidines against *Trypanosoma cruzi*. Antimicrob Agents Chemother 62:e02205-17. <https://doi.org/10.1128/AAC.02205-17>.

Copyright © 2018 American Society for Microbiology. All Rights Reserved.

Address correspondence to Maria de Nazaré C. Soeiro, soeiro@ioc.fiocruz.br.

TABLE 1 Trypanocidal activities, SIs, and I929 cytotoxicities of AIs against bloodstream trypomastigote and intracellular forms of *Trypanosoma cruzi*^a

Compound structure and name	Bloodstream forms (Y strain)		Intracellular forms (Tulahuen β -Gal strain)				I929 toxicity	
	EC ₅₀ (μ M) at:		EC ₅₀ (μ M) at 96 h		SI at 96 h		LC ₅₀ (μ M) at:	
	2 h	24 h	SI at 24 h	EC ₅₀ (μ M) at 96 h	SI at 96 h	24 h	96 h	
 2EVK008	4.83 (3.36–6.95)	1.21 (0.87–1.68)	20	2.04 (1.45–2.86)	7	24.75 (12.62–48.51)	14.33 (5.98–34.31)	
 27SMB078	30.67 (24.07–39.08)	0.46 (0.27–0.77)		7.78 (6.31–9.59)		ND	ND	
 28SMB032	44.61 (32.18–61.83)	10.48 (6.55–16.73)	>54	0.54 (0.41–0.70)	285	570.6 (364.0–894.7)	153.70 (98.42–240.10)	
 31DAP069	1.81 (1.45–2.24)	0.88 (0.65–1.19)	14	1.94 (1.36–2.76)	7	12.61 (6.58–24.15)	12.91 (5.26–31.71)	
 36DAP015	1.79 (1.40–2.30)	0.347 (0.26–0.45)	36	1.06 (0.625–1.81)	6	8.96 (4.41–18.20)	6.80 (2.95–15.68)	
 Bz	>50	9.76 (6.97–13.67)	>37	4.06 (3.61–4.56)	>89	>360	>360	

^aValues in parentheses are standard errors of the means for 95% confidence intervals. ND, not determined due to compound precipitation.

A	<i>T. cruzi</i> Y strain	CC	SI 48 h
	EC ₅₀ (μM) ^a 48 h	LC ₅₀ (μM) ^a 48 h	
28SMB032	1.59 (1.21-2.09)	304.4 (240.4-385.5)	191.44
Bz	1.58 (1.03-2.43)	>1000	633

FIG 1 (A) *In vitro* activities (EC₅₀s) and selectivity indices (SI) of 28SMB032 (A and C) and benznidazole (A and D) against intracellular forms of *T. cruzi* and the respective LC₅₀ upon primary cardiac cell (CC) cultures. (B to D) Light microscopy images of CC cultures infected with *T. cruzi* (Y strain) untreated (B) or exposed to 1.25 μM of 28SMB032 (C) and benznidazole (D). Original magnification, ×215. Values in parentheses are standard errors of the means for 95% confidence intervals.

parasite forms and strains. It is as active (EC₅₀, 1.59 μM; SI = 200) as Bz in cardiac cell cultures infected with the Y strain, and the Giemsa readout by light microscopy showed a trypanocidal effect rather than a trypanostatic effect, important to avoid parasite relapses (Fig. 1 and Table 1) (10, 11). The AIA combination with Bz assessed using a fixed-ratio method (12) gave a mean sum of fractional inhibitory concentration indexes (xΣFICI) of 0.95, conferring a status of no interaction (Table S1).

In silico adsorption, distribution, metabolism, excretion, and toxicity (ADMET) analysis and analysis with pan-assay interference compounds (PAINS) were done under different Web services: those of admetSAR (<http://lmmd.ecust.edu.cn:8000>), ACD/I-Lab, Pred-hERG (<http://labmol.com.br/predherg/>), PROTOX (<http://tox.charite.de/tox/>), and False Positive Remover (13–21). All compounds were predicted to be noncarcinogenic, nongenotoxic, non-human-ERG (hERG) blockers, and noninhibitors of most cytochrome P450 isoforms, besides having acceptable rodent toxicity by the oral route, moderate human intestinal absorption, and a favorable volume of distribution (Table S2). None contain PAINS substructures, and consequently, there is little probability that their biological activities are artifacts; they thus have a low probability of binding/inhibiting nonspecific targets (22).

For *in silico* prediction, a pool of potential targets in *T. cruzi* was generated. First, all three-dimensional (3D) structures available in the Protein Data Bank (PDB; <http://www.rcsb.org/pdb/>) with cocrystallized ligands were selected. Then, a bibliographic search with similar bioisosteric characteristics of the studied amidines was performed. Based on the concept that similar ligands bind to similar targets, three targets involved in the metabolism of putrescine or spermidine (23) and four known targets of pentamidine and analogues were identified. Homology models were built for trypanothione synthetase, POT1.1, POT1.2, and aquaporin (Fig. S2; Table S3). They were validated statistically using PROCHECK analysis (Fig. S3) (24). The overall stereochemical properties of the generated models are highly reliable and useful for a prospective target-fishing study. The final target pool is summarized in Table S4 and consisted of 30 potential targets, including enzymes and regulatory proteins. Molecular docking studies (Table 2) showed by the GlideScore energies the AIAs' high affinity to DNA, with energies ranging between −12.08 and −9.62 kcal/mol, which is next to that of pentamidine (−11.17 kcal/mol), a well-known DNA binder. Following in sequence of binding energy values were farnesyltransferase (PFT), spermidine synthase (SdpS), sterol 14- α demethylase (CYP51), and UDP-galactopyranose mutase (UGM). To explore earlier cellular insults induced by the AIAs, ultrastructural analysis was done on BT forms exposed for 2 h (using the EC₅₀ from 24 h) with the best fast killers, 31DAP069 and

TABLE 2 Docking score results of amidines with *T. cruzi* targets

Target candidate	EC ₅₀ (μM) ^a against bloodstream trypomastigotes (24 h at 37°C) with the ligand:				
	2EVK008 at 1.21 kcal/mol	27SMB078 at 0.46 kcal/mol	28SMB032 at 10.48 kcal/mol	31DAP069 at 0.88 kcal/mol	36DAP015 at 0.35 kcal/mol
DNA	-11.21	-10.14	-9.62	-11.45	-12.80
UDP-galactopyranose mutase	-8.27	-8.90	-4.38	-10.10	-7.15
Sterol 14- α demethylase	-9.76	-8.21	-7.25	-9.16	-8.74
Farnesyltransferase	-9.73	-7.66	-9.35	-8.51	-8.39
Spermidine synthase	-8.83	-9.48	-9.50	-8.11	-6.39
Pteridine reductase 2	-7.45	-7.49	-5.98	-7.69	-7.08
Trypanothione reductase	-6.91	-6.77	-5.51	-7.09	-8.21
Cruzain	-6.12	-6.22	-5.16	-6.95	-6.58
Phosphodiesterase	-7.06	-6.38	-5.29	-6.78	-7.20
POT1.1	-8.82	-6.28	-7.18	-6.50	-6.18
Acidocalcisomal pyrophosphatase	-6.20	-6.45	-6.93	-6.45	-5.37
Prostaglandin F2a synthase	-6.09	-5.69	-5.94	-6.27	-6.62
Farnesyl diphosphate synthase	-4.77	-7.06	-4.24	-6.23	-5.73
Glucokinase	-5.02	-7.63	-6.58	-6.23	-6.46
POT1.2	-5.47	-6.90	-6.57	-6.19	-6.27
Histidyl-tRNA synthetase	-5.86	-6.43	-6.79	-6.18	-5.43
Dihydrofolate reductase-thymidylate synthase	-6.47	-5.81	-7.94	-6.00	-6.74
Trans-sialidase	-6.90	-5.70	-6.14	-5.73	-5.73
Hypoxanthine phosphoribosyltransferase	-6.22	-5.57	-5.54	-5.68	-4.87
Trypanothione synthetase	-4.70	-5.11	-5.16	-5.32	-4.22
Glucose-6-phosphate isomerase	-3.66	-5.49	-5.02	-5.23	-4.11
Glyceraldehyde-3-phosphate dehydrogenase	-6.08	-4.66	-4.78	-4.96	-5.06
Triosephosphate isomerase	-5.93	-5.17	-5.44	-4.70	-4.13
Pyruvate kinase	-4.41	-4.29	-4.06	-4.45	-2.93
Dihydroorotate dehydrogenase	-4.64	-6.20	-4.67	-4.32	-4.21
Arginine kinase	-5.06	-5.00	-5.05	-4.26	-5.36
Ribose 5-phosphate isomerase type B	-3.93	-3.87	-4.50	-3.83	-3.25
Cyclophilin	-5.36	-3.81	-5.97	-3.59	-4.32
Superoxide dismutase	-4.54	-4.59	-5.83	-3.49	-4.53
Aquaporin	-3.05	-3.98	-4.23	-3.45	-4.29

^aBold values indicate the most probable targets according to score energies.

36DAP015, besides the most selective agent, 28SMB032. Scanning electron microscopy showed that 31DAP069 and 36DAP015 did not induce morphological modifications (Fig. 2B and C). Although most BTs exposed to 28SMB032 exhibited a profile similar to that of untreated ones (Fig. 2A1 and A2), some morphological alterations included shortening (Fig. 2D1 and D4) and twisting (Fig. 2D2 and D3) of the parasite bodies. Transmission electron microscopy (TEM) revealed that untreated parasites presented characteristic morphology (Fig. 3A1 and A2). BTs exposed to amidines exhibited similar cellular alterations regardless of the *in vitro* potency (EC₅₀s), including distension of the flagellar pocket, plasmatic and nuclear membrane dilation, distortions of the Golgi apparatus, the presence of concentric membranes and myelin figures, a large number of intracellular vesicles, and an altered profile of the endoplasmic reticulum surrounding cytoplasmic components (Fig. 3B1 to D8), suggestive of an autophagy phenotype that deserves further analysis.

Literature data demonstrate that classical amidines, such as pentamidine (25) and some analogues (26), strongly interact with DNA in a binding mode very similar to those of hydrophobic methylene groups and with rings tightly bound to the minor groove. Additionally, findings revealed that although some of the most active AIAs were not good DNA binders, some AIAs strongly altered DNA topology, impairing functionality (27). Even the fast and potent AIAs did not induce ultrastructural alterations of the DNA, and it may be possible that TEM is not sensitive enough for detecting minor topology alterations detected *in silico* and/or that there is a lack of translation among *in silico* and whole-cell-based assays. In order to deeply explore the binding mode and effect, thermodynamic studies are needed. Plus, the observed *in vitro* activity can involve other predicted targets, such as UGM, CYP51, PFT, and SdpS, related to *T. cruzi* fitness and pathogenesis; some of their inhibitors, such as the CYP51 inhibitors

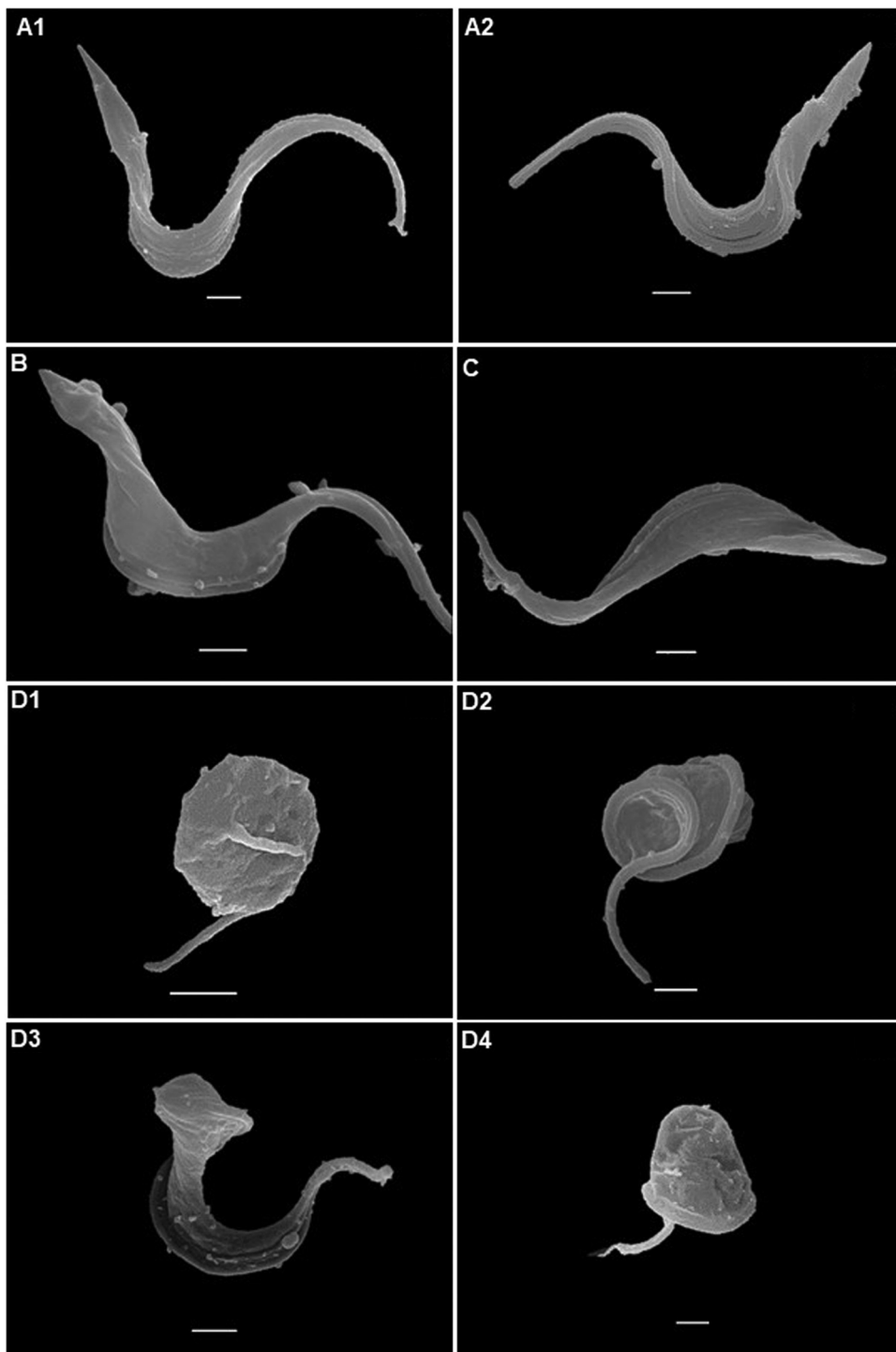


FIG 2 Scanning electron microscopy examination of *T. cruzi* bloodstream trypomastigotes (Y strain). (A) Control with no compound exposure. Treatment with 0.88 μM 31DAP069 (B), 0.35 μM 36DAP015 (C), and 10.48 μM 28SMB032 (D) resulted in no morphological alteration for the parasites shown in panel B or C, but the parasites in panels D1 to D4 exhibited body retraction, and those in panels D2 and D3 exhibited a twist of the parasite body. Bars = 1 μm .

recently assayed in clinical trials for the chronic stage of CD, are considered anti-*T. cruzi* drug candidates (28), but again, their potency in preclinical studies did not translate into clinical outcomes (29, 30).

Our findings corroborate previous studies related to the potent *in vitro* activities of

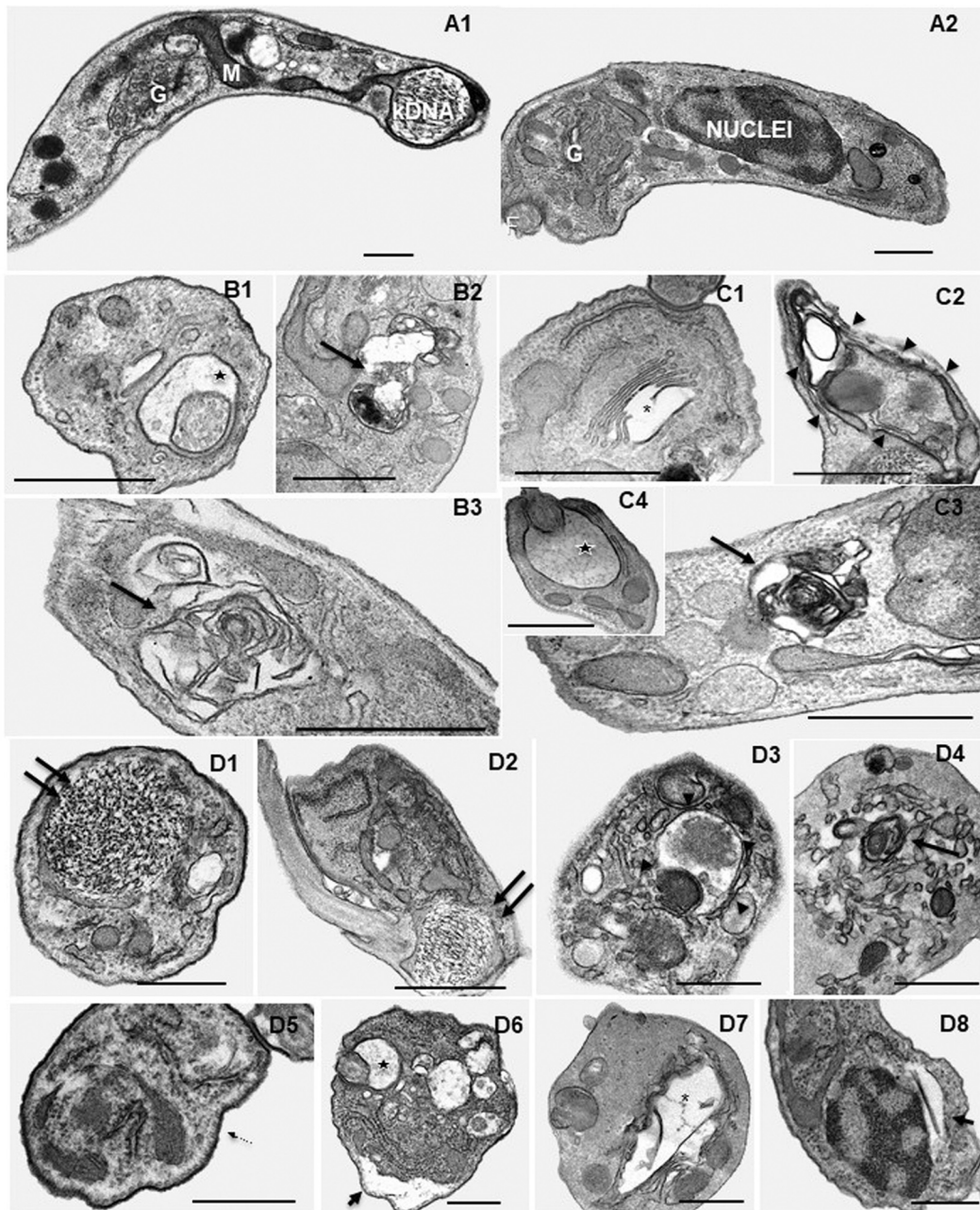


FIG 3 Ultrastructural effects of AIAs in *T. cruzi* bloodstream trypomastigotes (Y strain). (A1 and A2) Controls with no compound exposure display the characteristic morphology. Treatment with 0.88 μM 31DAP069 (panels B), 0.35 μM 36DAP015 (panels C), and 10.48 μM 28SMB032 (panels D) resulted in several insults, including dilatation of the flagellar pocket (black star in panels B1, C4, and D6), concentric membranar structures and myelin figures in the cytosol (black arrows in panels B2, B3, C3, and D4), disruption of the Golgi apparatus (asterisk in panels C1 and D7), an endoplasmic reticulum surrounding cytosolic structures (arrowheads in panels C2 and D3), and detachment of the nuclear (short arrow in panel D8) and plasma (short arrow in panel D6) membranes. No alterations were detected in subpellicular microtubules (thin arrows in panel D5) and on the parasite kinetoplast DNA (kDNA) (double arrows in panels D1 and D2). G, Golgi cisternae; M, mitochondria; N, nuclei; F, flagellum. Bars = 500 nm.

AIAs against intracellular trypanosomatids meeting the expectations of a hit compound (an EC_{50} of $<10 \mu\text{M}$ and an SI of at least 10) (31) and having a favorable pharmacokinetic profile. All of this background encouraged us to conduct *in vivo* assays. 28SMB032 was moved to an *in vivo* assay using a mouse (male Swiss Webster, 18 to 20 g) model of acute infection (10^4 BTs from the Y strain) under different compound concentrations (10 to 0.1 mg/kg of body weight) diluted with two vehicles (0.5%

carboxymethylcellulose and 10% dimethyl sulfoxide [DMSO]), given intraperitoneally (i.p.) and orally (p.o.). Animals were handled ethically (CEUA Fiocruz protocol number LW-16/14). Mice with confirmed parasitemia were treated (with single and combined therapy) at the 5th and 8th days postinfection (p.i.), which in this experimental model correspond to the times of parasitemia onset and peak, respectively (32). Regardless of the vehicle, 0.1 mg/kg 28SMB032 given i.p. and p.o. did not reduce the mortality rates induced by parasite infection. 28SMB032 alone (10 and 1 mg/kg, i.p., DMSO) or combined with Bz (p.o.) showed a toxic profile, leading to >83% of the animals dying less than 24 h after drug administration. Gross pathology showed a large amount of yellow deposits of the AIA at the peritoneum as well as gastrointestinal bleeding and signs of acute renal failure with kidney atrophy (data not shown). However, this AIA, given as monotherapy at 0.1 mg/kg (i.p., with DMSO as the vehicle), led to a 40% reduction of the parasite load at the peak (8 days p.i.). Although *in vitro* outcomes did not fully translate in the experimental animal models, the molecule optimization may reduce the toxicity issues of this class of compounds and contribute to alternative treatments for CD.

SUPPLEMENTAL MATERIAL

Supplemental material for this article may be found at <https://doi.org/10.1128/AAC.02205-17>.

SUPPLEMENTAL FILE 1, PDF file, 2.9 MB.

ACKNOWLEDGMENTS

The present study was supported by grants from the Fundação Carlos Chagas Filho de Amparo à Pesquisa do Estado do Rio de Janeiro (FAPERJ), Conselho Nacional Desenvolvimento Científico e Tecnológico (CNPq), Coordenação de Aperfeiçoamento de Pessoal de Nível Superior (CAPES), Fundação Oswaldo Cruz, PDTIS, PAEF/CNPq/Fiocruz, and CAPES. We thank the Fortalecimento dos Programas de Gestão Estratégica de Pesquisa da Fiocruz Rede de Plataformas Fiocruz (grant VPPLR-001-Fio 14) and the Programa de Excelência Acadêmica (PROEX) from CAPES. M.D.N.C.S. is a research fellow of the CNPq and a CNE researcher.

REFERENCES

- World Health Organization. 2013. Sustaining the drive to overcome the global impact of neglected tropical diseases: second WHO report on neglected tropical diseases. World Health Organization, Geneva, Switzerland.
- Pecoul B, Batista C, Stobbaerts E, Ribeiro I, Vilasanjuan R, Gascon J, Pinazo MJ, Moriana S, Gold S, Pereiro A, Navarro M, Torrico F, Bottazzi MF, Hotez PJ. 2016. The BENEFIT trial: where do we go from here? *PLoS Negl Trop Dis* 10:e0004343. <https://doi.org/10.1371/journal.pntd.0004343>.
- Wilkinson SR, Taylor MC, Horn D, Kelly JM, Cheeseman L. 2008. A mechanism for cross-resistance to nifurtimox and benznidazole in trypanosomes. *Proc Natl Acad Sci U S A* 105:5022–5027. <https://doi.org/10.1073/pnas.0711014105>.
- Soeiro MDNC, Werbovetz K, Boykin DW, Wilson WD, Wang MZ, Hemphill A. 2013. Novel amidines and analogues as promising agents against intracellular parasites: a systematic review. *Parasitology* 140:929–951. <https://doi.org/10.1017/S0031182013000292>.
- Patrick DA, Ismail MA, Arafa RK, Wenzler T, Zhu X, Pandharkar T, Jones SK, Werbovetz KA, Brun R, Boykin DW, Tidwell RR. 2013. Synthesis and antiprotozoal activity of dicationic m-terphenyl and 1,3-dipyridylbenzene derivatives. *J Med Chem* 56:5473–5494. <https://doi.org/10.1021/jm400508e>.
- Wu C, Wei J, Tian D, Feng Y, Miller RH, Wang Y. 2008. Molecular probes for imaging myelinated white matter in CNS. *J Med Chem* 51:6682–6688. <https://doi.org/10.1021/jm8003637>.
- Musante C. 1951. Some derivatives of pyrazole and isoxazole having antituberculous action. *Farmacologia* 6:32–38.
- Stephens CE, Tanious F, Kim S, Wilson WD, Schell WA, Perfect JR, Franzblau SG, Boykin DW. 2001. Diguandino and “reversed” diamidino 2,5-diarylfurans as antimicrobial agents. *J Med Chem* 44:1741–1748. <https://doi.org/10.1021/jm000413a>.
- Romanha AJ, De Castro SL, Soeiro MNC, Lannes-Vieira J, Ribeiro I, Talvani A, Bourdin B, Blum B, Olivieri B, Zani C, Spadafora C, Chiari E, Chatelain E, Chaves G, Calzada JE, Bustamante JM, Freitas-Junior LH, Romero LI, Bahia MT, Lotrowska M, Soares M, Andrade SG, Armstrong T, Degraive W, Andrade ZA. 2010. *In vitro* and *in vivo* experimental models for drug screening and development for Chagas disease. *Mem Inst Oswaldo Cruz* 105:233–238. <https://doi.org/10.1590/S0074-02762010000200022>.
- Ercoli N, Ludice G. 1980. Trypanostatic drug action: its relation to relapse following chemotherapy. *Chemotherapy* 26:218–223. <https://doi.org/10.1159/000237908>.
- Cal M, Ioset J-R, Fügi MA, Mäser P, Kaiser M. 2016. Assessing anti-*T. cruzi* candidates *in vitro* for sterile cidal activity. *Int J Parasitol Drugs Drug Resist* 6:165–170. <https://doi.org/10.1016/j.ijpddr.2016.08.003>.
- Fivelman QL, Adagu IS, Warhurst DC. 2004. Modified fixed-ratio isobologram method for studying *in vitro* interactions between atovaquone and proguanil or dihydroartemisinin against drug-resistant strains of *Plasmodium falciparum*. *Antimicrob Agents Chemother* 48:4097–4102. <https://doi.org/10.1128/AAC.48.11.4097-4102.2004>.
- Cheng F, Li W, Zhou Y, Shen J, Wu Z, Liu G, Lee PW, Tang Y. 2012. AdmetSAR: a comprehensive source and free tool for assessment of chemical ADMET properties. *J Chem Infect Model* 52:3099–3105. <https://doi.org/10.1021/ci300367a>.
- Lagunin A, Filimonov D, Zakharov A, Xie W, Huang Y, Zhu F, Shen T, Yao J, Poroikov V. 2009. Computer-aided prediction of rodent carcinogenicity by PASS and CISOC-PSCT. *QSAR Comb Sci* 28:806–810. <https://doi.org/10.1002/qsar.200860192>.
- Hansen K, Mika S, Schroeter T, Sutter A, ter Laak A, Steger-Hartmann T, Heinrich N, Müller KR. 2009. Benchmark data set for *in silico* prediction

- of Ames mutagenicity. *J Chem Infect Model* 49:2077–2081. <https://doi.org/10.1021/ci900161g>.
16. Shen J, Cheng F, Xu Y, Li W, Tang Y. 2010. Estimation of ADME properties with substructure pattern recognition. *J Chem Infect Model* 50:1034–1041. <https://doi.org/10.1021/ci100104j>.
 17. Cheng F, Yu Y, Shen J, Yang L, Li W, Liu G, Lee PW, Tang Y. 2011. Classification of cytochrome P450 inhibitors and noninhibitors using combined classifiers. *J Chem Infect Model* 51:996–1011. <https://doi.org/10.1021/ci200028n>.
 18. Braga RC, Alves VM, Silva MF, Muratov E, Fourches D, Tropsha A, Andrade CH. 2014. Tuning hERG out: antitarget QSAR models for drug development. *Curr Top Med Chem* 14:1399–1415. <https://doi.org/10.2174/1568026614666140506124442>.
 19. Braga RC, Alves VM, Silva MFB, Muratov E, Fourches D, Lião LM, Tropsha A, Andrade CH. 2015. Pred-hERG: a novel Web-accessible computational tool for predicting cardiac toxicity. *Mol Inform* 34:698–701. <https://doi.org/10.1002/minf.201500040>.
 20. Drwal MN, Banerjee P, Dunkel M, Wettig MR, Preissner R. 2014. ProTox: a web server for the in silico prediction of rodent oral toxicity. *Nucleic Acids Res* 42:W53–W58. <https://doi.org/10.1093/nar/gku401>.
 21. Baell JB, Holloway GA. 2010. New substructure filters for removal of pan assay interference compounds (PAINS) from screening libraries and for their exclusion in bioassays. *J Med Chem* 53:2719–2740. <https://doi.org/10.1021/jm901137j>.
 22. Biasini M, Bienert S, Waterhouse A, Arnold K, Studer G, Schmidt T, Kiefer F, Gallo Cassarino T, Bertoni M, Bordoli L, Schwede T. 2014. SWISS-MODEL: modelling protein tertiary and quaternary structure using evolutionary information. *Nucleic Acids Res* 42:W252–W258. <https://doi.org/10.1093/nar/gku340>.
 23. Maya JD, Salas CO, Aguilera-Venegas B, Diaz MV, López-Muñoz R. 2014. Key proteins in the polyamine-trypanothione pathway as drug targets against *Trypanosoma cruzi*. *Curr Med Chem* 21:1757–1771. <https://doi.org/10.2174/0929867320666131119122145>.
 24. Laskowski RA, MacArthur MW, Moss DS, Thornton JM. 1993. PROCHECK: a program to check the stereochemical quality of protein structures. *J Appl Crystallogr* 26:283–291. <https://doi.org/10.1107/S0021889892009944>.
 25. Nunn CM, Jenkins TC, Neidle S. 1993. Crystal structure of d(CGCGAATT CGCG) complexed with propamidine, a short-chain homologue of the drug pentamidine. *Biochemistry* 32:13838–13843. <https://doi.org/10.1021/bi00213a012>.
 26. Chai Y, Munde M, Kumar A, Mickelson L, Lin S, Campbell NH, Banerjee M, Akay S, Liu Z, Farahat AA, Nhili R, Depauw S, David-Cordonnier MH, Neidle S, Wilson WD, Boykin DW. 2014. Structure-dependent binding of arylimidamides to the DNA minor groove. *Chembiochem* 15:68–79. <https://doi.org/10.1002/cbic.201300622>.
 27. Daliry A, Pires MQ, Silva CF, Pacheco RS, Munde M, Stephens CE, Kumar A, Ismail MA, Liu Z, Farahat AA, Akay S, Som P, Hu Q, Boykin DW, Wilson WD, De Castro SL, Soeiro MDNC. 2011. The trypanocidal activity of amidine compounds does not correlate with their binding affinity to *Trypanosoma cruzi* kinetoplast DNA. *Antimicrob Agents Chemother* 55:4765–4773. <https://doi.org/10.1128/AAC.00229-11>.
 28. Pereira-Chioccola VL, Acosta-Serrano A, Correia de Almeida I, Ferguson MA, Souto-Padron T, Rodrigues MM, Travassos LR, Schenkman S. 2000. Mucin-like molecules form a negatively charged coat that protects *Trypanosoma cruzi* trypomastigotes from killing by human anti-alpha-galactosyl antibodies. *J Cell Sci* 113:1299–1307.
 29. Urbina JA. 2015. Recent clinical trials for the etiological treatment of chronic Chagas disease: advances, challenges and perspectives. *J Eukaryot Microbiol* 62:149–156. <https://doi.org/10.1111/jeu.12184>.
 30. Molina I, Salvador F, Sánchez-Montalvá A. 2015. The use of posaconazole against Chagas disease. *Curr Opin Infect Dis* 28:397–407. <https://doi.org/10.1097/QCO.0000000000000192>.
 31. Katsuno K, Burrows JN, Duncan K, Hooft van Huijsduijnen R, Kaneko T. 2015. Hit and lead criteria in drug discovery for infectious diseases of the developing world. *Nat Rev Drug Discov* 14:751–758. <https://doi.org/10.1038/nrd4683>.
 32. Batista DDGJ, Batista MM, Oliveira GM, Amaral PB, Lanes-Vieira J, Britto C, Junqueira A, Lima MM, Romanha AJ, Sales Junior PA, Stephens CE, Boykin DW, Soeiro MDNC. 2010. Arylimidamide Db766: a potential chemotherapeutic candidate for Chagas disease treatment. *Antimicrob Agents Chemother* 54:2940–2952. <https://doi.org/10.1128/AAC.01617-09>.